NASA TECHNICAL MEMORANDUM

NASA TM X-3176

NASA TM X-3176

# GROUND IDLE PERFORMANCE IMPROVEMENT OF A DOUBLE-ANNULAR COMBUSTOR BY USING SIMULATED VARIABLE COMBUSTOR GEOMETRY

*Donald F. Schultz*

*Lewis Research Center*
*Cleveland, Ohio 44135*

NATIONAL AERONAUTICS AND SPACE ADMINISTRATION • WASHINGTON, D. C. • FEBRUARY 1975

| 1. Report No. NASA TM X-3176 | 2. Government Accession No. | 3. Recipient's Catalog No. |
|---|---|---|
| 4. Title and Subtitle GROUND IDLE PERFORMANCE IMPROVEMENT OF A DOUBLE-ANNULAR COMBUSTOR BY USING SIMULATED VARIABLE COMBUSTOR GEOMETRY | | 5. Report Date February 1975<br>6. Performing Organization Code |
| 7. Author(s) Donald F. Schultz | | 8. Performing Organization Report No. E-8097<br>10. Work Unit No. 505-04 |
| 9. Performing Organization Name and Address Lewis Research Center<br>National Aeronautics and Space Administration<br>Cleveland, Ohio 44135 | | 11. Contract or Grant No.<br>13. Type of Report and Period Covered Technical Memorandum |
| 12. Sponsoring Agency Name and Address National Aeronautics and Space Administration<br>Washington, D.C. 20546 | | 14. Sponsoring Agency Code |

15. Supplementary Notes

16. Abstract

A test program was undertaken to determine if variable combustor geometry could be used to reduce exhaust emissions of a low-pressure-ratio jet engine operating at ground idle conditions. Three techniques for varying combustor geometry were simulated. Other techniques evaluated were radial fuel staging and the use of preheated fuel. When simulated variable combustor geometry was employed with radial fuel staging, combustion efficiency at a fuel-air ratio of 0.01 was increased from 77 to 95 percent, and exhaust emissions of unburned hydrocarbons and carbon monoxide were significantly reduced.

| 17. Key Words (Suggested by Author(s)) | 18. Distribution Statement |
|---|---|
| Jet engine<br>Combustor<br>Annular<br>Variable geometry<br>Combustion efficiency<br>Exhaust emissions | Unclassified - unlimited<br>STAR Category 25 (rev.) |

| 19. Security Classif. (of this report) | 20. Security Classif. (of this page) | 21. No. of Pages | 22. Price* |
|---|---|---|---|
| Unclassified | Unclassified | 32 | $3.25 |

* For sale by the National Technical Information Service, Springfield, Virginia 22151

# GROUND IDLE PERFORMANCE IMPROVEMENT OF A DOUBLE-ANNULAR COMBUSTOR BY USING SIMULATED VARIABLE COMBUSTOR GEOMETRY

by Donald F. Schultz

Lewis Research Center

## SUMMARY

A test program was undertaken to determine if variable combustor geometry could be used to reduce exhaust emissions of a low-pressure-ratio jet engine operating at ground idle conditions. Three techniques for varying combustor geometry were simulated. They included use of a simulated translating outer exit transition liner, simulated flapper valves on the combustor snout inlet, and a simulated distorted diffuser inlet-air velocity profile. All these modes were designed to increase combustion efficiency by passing air around the primary zone and thus reducing the reference velocity in the primary combustion zone. Other techniques for improving engine ground idle combustion efficiency that were evaluated were radial fuel staging and use of preheated fuel.

When simulated variable combustor geometry was employed with radial fuel staging, combustion efficiency at a fuel-air ratio of 0.01 was increased from 77 to 95 percent, and exhaust emissions of unburned hydrocarbons and carbon monoxide were significantly reduced. Fuel preheated to 410 K increased combustion efficiency as much as 12.8 percent at low efficiencies but had little effect when combustion efficiencies were greater than 90 percent.

## INTRODUCTION

A test program was undertaken to determine if variable combustor geometry would improve the ground idle performance, and thus reduce exhaust emissions, of a double-annular combustor operating at a simulated ground idle condition com-

parable to that of a low-pressure-ratio fan or turbojet engine. In order to meet the 1979 Environmental Protection Agency standards for carbon monoxide and unburned hydrocarbons (ref. 1), engines must idle with combustion efficiencies in excess of 99 percent. At present no low-compression-ratio engine has an idle combustion efficiency near 99 percent. Combustion efficiency is low at the low-compression-ratio idle condition because of the low combustor inlet pressures and temperatures encountered at this condition (typically of the order of 2 atm and 370 K, at fuel-air ratios of 0.008 to 0.012). These severe operating conditions result in high emission of carbon monoxide and unburned hydrocarbons.

Previous work in this area is described in reference 2, which discusses the effects of fuel nozzle spray angle, radial fuel staging, and axial as opposed to radial inflow air swirlers. Reference 3 shows the benefits of air-atomizing splash-cone fu nozzles in reducing idle emissions. The investigation described in this report went a step beyond previous work by using variable combustor geometry to reduce primary-zone reference velocity in an effort to reduce exhaust emissions of carbon monoxide and unburned hydrocarbons, which are a function of reference velocity. In addition, the variable-geometry techniques employed increased the primary-zone fuel-air ratio and thus raised the primary-zone average temperature. This higher temperature in turn reduced emissions of carbon monoxide and unburned hydrocarbons. Six variable-geometry configurations were tested as well as the unmodifie combustor.

All configurations were full-annular combustors. The simulated variable-combustor-geometry techniques were all designed to bypass air around the primary zone of the combustor. Techniques investigated included use of a simulated translating combustor exit transition liner, simulated flapper valves on the combustor snout inlet, and a simulated distorted diffuser inlet-air velocity profile. Radial fuel staging was employed as well as fuel heated to 410 K. No attempt was made to build any functional variable-geometry hardware. These tests were conducted at an inlet total pressure of 20.2 newtons per square centimeter, an inlet temperature of 378 K, a reference velocity of 22.7 meters per second, and overall fuel-air ratios of 0.008 to 0.012.

## APPARATUS AND PROCEDURE

### Test Combustor

Combustor design. - The combustor used in this program is referred to as a double-annular, ram-induction combustor. It was designed for Mach 3.0 cruise operation. The double-annular design permits a considerable reduction in combustor length while maintaining an adequate ratio of length to annulus height. The ram-induction principle utilizes the kinetic energy of the inlet air to provide rapid mixing both in the primary zone and in the secondary zone. The advantages of this combustor are a shorter combustor length, a shorter diffuser length, a reduction in the film-cooling-air requirement, and radial fuel staging capability. A cross-sectional sketch of the combustor in its nonidle configuration may be seen in figure 1. Figure 2 shows photographs of the combustor in this configuration. The combustor has 64 fuel nozzles, 32 in each annulus. One size of simplex fuel nozzle was used. The fuel flow from each nozzle was 7.71 kilograms per hour, ±2 percent, with a fuel nozzle differential pressure of 103.4 newtons per square centimeter.

The combustor has two igniters located in the outer annulus, 180° apart. Each igniter was supplied by a 20-joule capacitance discharge power supply. References 2, 4 to 6, and 12 supply additional details of combustor design and performance.

Combustor configurations. - Six combustor configurations plus the unmodified combustor were tested in all. Table I is a summary of the configurations tested. The primary variable-geometry concept tested for improving engine ground idle performance was a simulated translating outer exit transition liner section. Figure 3 shows inside and outside views of this simulated translating liner in the open or engine idle mode. Three other modifications were used to complement this concept. These were variable combustor snout blockage, simulated by welding punched plates across the snout inlet as shown in figure 4; a distorted diffuser inlet profile, which would be made into a uniform profile during other engine operating conditions by use of diffuser bleed (ref. 7); and the use of axial-flow or radial-inflow air swirlers. Figure 5 shows the inlet distortion plates installed in the combustor diffuser inlet and a plot of the resulting inlet-air velocity profile.

Figure 5(c), a plot of the inlet-air velocity profiles used, is for a simulated takeoff condition rather than idle; however, the inlet Mach number is about the same

(0.243 for takeoff compared with 0.221 for the idle condition). Naturally the inlet pressure and temperature at takeoff are also higher than at idle, but they have little effect on the velocity profile.

The axial-flow and radial-inflow air swirlers used in these tests are shown in figure 6. The three best configurations and the original are shown in cross section in figure 7. In each configuration the primary technique employed to increase combustion efficiency, and thus reduce exhaust emissions, was to reduce the effective primary-zone reference velocity by passing air around the primary and secondary combustion zones and dumping this bypassed air into the combustor at the upstream end of the outer exit transition liner. The punched plate on the combustor snout and the inlet-airflow distortion plate increased the bypass flow and thus further reduced the effective combustor reference velocity. Radial fuel staging was also employed. With radial fuel staging the entire fuel flow is supplied to only one annulus, and thus twice as much fuel is introduced into each fuel nozzle for the same overall fuel-air ratio. The higher fuel flows require higher fuel nozzle differential pressures, which result in better fuel atomization. Other performance improvements due to radial fuel staging are documented in reference 6. Both radial-inflow and axial-flow air swirlers were also tested, since the type of air swirler can significantly affect the mixing of air and fuel (ref. 2).

## Test Conditions

All testing was done at test conditions simulating operation of a low-pressure-ratio engine. An inlet-air total pressure of 20.2 newtons per square centimeter, temperature of 378 K, and reference velocity of 22.7 meters per second were used. The fuel-air ratio was varied from 0.008 to 0.012. The fuel temperature was ambient except for a few test points taken with fuel heated to 410 K. Table II is a listing of the test data obtained.

## Testing Procedure

All variable-geometry combustor configurations were simulated by using fixed geometry hardware to simplify testing and configuration changes. When the required

inlet-air conditions were attained, fuel was supplied first to both annuli and then to either the inner or outer annulus only. In each case the overall fuel-air ratio was varied from 0.008 to 0.012. However, with single-annulus operation a 0.012 fuel-air ratio was unobtainable because the single set of simplex fuel nozzles used in these tests could not accommodate the required fuel flow within the fuel pressure limit of the fuel system.

## Test Facility

This research program was conducted in a closed-duct test facility at the Lewis Research Center. A schematic of this facility is shown in figure 8. Airflow rates for combustion from 2.3 to 136 kilograms per second could be obtained. Pressures from 1.7 to 113.8 newtons per square centimeter could be obtained. Air temperature could be controlled over a range of 265 to 922 K without vitiation before entering the combustor.

Fuel was available for the tests at temperatures from ambient to 410 K and at pressures up to 700 newtons per square centimeter. A 79-newton-per-square-centimeter steam heat exchanger was used for indirectly heating the fuel.

## Instrumentation

Measurements to determine combustor operation and performance were recorded by the Lewis central automatic data processing system (ref. 8). Control-room readout instrumentation (indicating and recording) was used to set and monitor the test conditions and the operation of the combustor. Pressures were measured and recorded by the central digital automatic multiple pressure recorder and by strain-gage pressure transducers (ref. 9). Iron-constantan thermocouples were used to measure temperatures between 240 to 675 K, and Chromel-Alumel thermocouples measured temperatures between 240 and 1560 K. High temperatures, to 1920 K, were measured with platinum-13-percent-rhodium - platinum thermocouples. The indicated readings of all thermocouples were taken as true values of the total temperatures. The platinum-13-percent-rhodium - platinum thermocouples were of the high-recovery aspirating type (ref. 10, type 6).

Airflow rates were measured by square-edge orifices installed according to ASME specifications. Fuel-flow rates were measured by turbine flowmeters with frequency-

to-voltage converters for readout and recording.

The axial locations of the combustor instrumentation stations along the test section are shown in figure 5 (a). Instrumentation at inlet station 3 is shown in figure 9. Inlet-air temperature was measured by eight Chromel-Alumel thermocouples equally spaced around the inlet at station 3. Inlet-air total-pressure was measured by eight five-point total-pressure rakes equally spaced around the inlet at station 3. The pressure rakes measured the total-pressure profile at centers of equal areas across the inlet annulus. Static pressure at the inlet was measured by 16 wall static-pressure taps, 8 on the outside and 8 on the inside walls of the annulus. The diffuser inlet velocity profile was measured by four five-point pitot-static tube rakes located at station 3.5.

Combustor outlet total temperature and pressure at instrumentation station 4 were measured at $3^{\circ}$ increments around the exit circumference. At each $3^{\circ}$ increment five temperatures and pressures were measured across the annulus. The sensors were located at centers of equal areas across the annulus. The water-cooled probe assembly containing the five temperature and pressure sensors is shown in figure 10. Three of these probes, each on an arm $120^{\circ}$ from the others, rotated $120^{\circ}$ and provided full coverage of the circumference. Water-cooled shields protected the probes when not in use at three fixed points in the exhaust stream. Temperature and pressure were not measured at these points. The probes were made of platinum-rhodium alloy where exposed to the hot exhaust gases. Also located at station 4 were eight wall static-pressure taps and four randomly spaced five-point fixed steam-cooled gas sample probes which were used for most gas samples. Late in the program three five-point rotating gas sample probes were used in place of the fixed probes. In all cases all the gas sample probes were manifolded together before the analysis was made.

## Calculations

Combustion efficiency by thermocouple measurement. - Efficiency was determined by dividing the measured temperature rise across the combustor by the theoretical temperature rise. The theoretical rise was calculated from the fuel-air ratio, fuel properties, inlet-air temperature and pressure, and the amount of water vapor present in the inlet airflow. The exit temperatures were measured with five-point

raversing aspirated thermocouple probes and were mass weighted for the efficiency alculation. The indicated readings of all thermocouples were taken as true values f the total temperatures. The mass-weighting procedure is given in reference 11. n each mass-weighted average, 585 individual exit temperatures were used.

Combustion efficiency by exhaust gas analysis. - Efficiency was determined by neasuring the exhaust products carbon dioxide, carbon monoxide, and unburned ydrocarbons. Multiple gas samples were obtained as described in the section nstrumentation. An analysis was made 39 times for each data point. The derived ombustion efficiency was validated by determining the combustor fuel-air ratio from he exhaust analysis. This fuel-air ratio was divided by the metered fuel-air ratio o compare their agreement. Values of this ratio of fuel-air ratios of $1.0 \pm 0.05$ were onsidered acceptable. Most values fell in this range (table II).

Reference velocity and diffuser inlet Mach number. - Reference velocity $V_{ref}$ or the combustor was computed from the total airflow, the diffuser inlet total pres- ure and temperature, and the maximum cross-sectional area between the inner and uter shrouds. Diffuser inlet Mach number was calculated from the total airflow, he total temperature and the static pressure measured at the diffuser inlet, and the nlet annulus area.

Total-pressure loss. - The total-pressure loss $\Delta P/P$ was calculated by mass veraging total pressures measured upstream of the diffuser inlet and at the com- ustor exit. The total-pressure loss, therefore, included the diffuser loss.

Diffuser inlet velocity profile. - The diffuser inlet velocity profile was deter- ined by calculating the average position velocity at each of the five radial positions rom data taken by the four pitot-static tube rakes at station 3.5.

## Units

The U.S. customary system of units was used for primary measurements and alculations. Values were converted to SI units (Systeme International d'Unités) or reporting purposes only. When the conversions were made, consideration was iven to implied accuracy, so that some of the values expressed in SI units were ounded off.

## RESULTS AND DISCUSSION

Figures 11 to 13 illustrate the effects of simulated variable combustor geometry combined with radial fuel staging. Combustion efficiency and exhaust emissions of carbon monoxide, unburned hydrocarbons, and oxides of nitrogen are discussed in this section along with supplementary data related to exit temperature profile, total-pressure loss, the use of fuel preheated to 410 K, and durability.

### Combustion Efficiency

Combustion efficiency was determined by exhaust gas analysis and verified by thermocouple measurement. All data figures were prepared by using the gas-analysis measurements.

Figure 11(a) compares combustion efficiency as a function of fuel-air ratio with combustion in the inner annulus only for the unmodified and three variable-geometry combustor configurations. Since all the fuel was supplied to only one annulus, the local fuel-air ratio in the annulus was double that which would exist if fuel were supplied to both annuli. Substantial improvements in combustion efficiency were obtained at all fuel-air ratios by employment of variable geometry with radial fuel staging. A combustion efficiency of 95.2 percent was obtained with model 6C (model with short liner and inlet-air distortion). This compares with only 88.6 percent for model 6A (unmodified model) at a similar fuel-air ratio. A 6.6-percentage-point improvement in combustion efficiency was obtained by using variable combustor geometry. The inlet-airflow distortion, which simulates a tip-peaked compressor flow in model 6C, diverts more air around the outer annulus to the simulated translated outer exit transition liner. This air diversion further reduces the effective reference velocity in the inner annulus and increases combustion efficiency.

At an idle fuel-air ratio of about 0.008, however, model 6D (model with short liner, snout blockage, and axial-flow rather than radial-inflow air swirlers) outperformed model 6C by attaining 95.1 percent combustion efficiency compared with 93.2 percent for model 6C, as shown in figure 11(a).

Figure 11(b) shows combustion efficiency as a function of overall fuel-air ratio with combustion in the outer annulus only. Model 6C performed best by attaining a combustion efficiency of 95.3 percent at a fuel-air ratio of 0.0101. Model 6D was

not tested with combustion in the outer annulus only because of liner durability problems encountered while testing models 6B and 6C.

For comparative purposes figure 11(c) shows combustion efficiency as a function of fuel-air ratio for the four combustors with combustion in both annuli. Comparing figures 11(a) and (c) shows that a 19.2-percentage-point increase in combustion efficiency was obtained by using model 6C (model with short liner and inlet-air distortion) with combustion in the inner annulus only compared with model 6A (unmodified model) with combustion in both annuli at a fuel-air ratio of 0.0096. The fuel-air-ratio range covered with single-annulus burning was narrower than that with burning in both annuli because of the limited fuel-flow range of the simplex fuel nozzles.

In all three modes of operation, combustion in both annuli, inner annulus only, or outer annulus only, substantial improvements in combustion efficiency were obtained by using variable-combustor-geometry techniques.

## Exhaust Emissions

Unburned hydrocarbons. - Figure 12 shows the unburned-hydrocarbon emission index as a function of fuel-air ratio and the effects of radial fuel staging for the different variable-geometry combustor models tested. Figure 12(a) shows a substantial reduction in unburned-hydrocarbon emission index as fuel-air ratio was increased from 0.008 to 0.01 for all models. Of course, this improvement is reflected in the efficiency data shown in figure 11. In addition, figure 12(a) shows a dramatic reduction in unburned hydrocarbons by the use of variable combustor geometry. Model 6C (model with short liner and inlet-air distortion) had an emission index of only 24 grams per kilogram of fuel at a fuel-air ratio of 0.0096 compared with 75 grams per kilogram of fuel for model 6A (unmodified model). Comparing figures 12(a) to (c) shows that the greatest reduction in unburned-hydrocarbon emission index occurred with model 6C with combustion in either annulus (values as low as 24 g/kg fuel in both cases).

Comparing figures 12(a) and (c) shows that a 93-percent decrease in unburned-hydrocarbon emission index was obtained by using model 6C with outer-annulus burning only compared with model 6A with burning in both annuli at an overall fuel-air ratio of 0.008. Thus, model 6C provides a substantial reduction in unburned-

hydrocarbon emission index. In this case (fig. 12(b)) variable combustor geometry reduces unburned-hydrocarbon emission index an additional 43 percent from that obtained by using radial fuel staging only.

Carbon monoxide. - Figure 13 shows carbon monoxide emission index as a function of fuel-air ratios and shows the effect of radial fuel staging for the different variable-geometry combustors tested. Carbon monoxide emission index decreased with increasing fuel-air ratio except with model 6B (model with short liner and snou blockage) when radial fuel staging was used with combustion in the outer annulus only. In this case (fig. 13(b)) carbon monoxide emission index increased from 103 to 114 grams per kilogram of fuel while fuel-air ratio increased from 0.008 to 0.01. Figure 13(a) shows a carbon monoxide emission index of 91 grams per kilogram of fuel for model 6D (model with short liner, snout blockage, and axial-flow air swirlers) at a fuel-air ratio of 0.0095 with combustion in the inner annulus only. This value compares with a carbon monoxide emission index of 169 grams per kilogram of fuel for model 6A (unmodified model) at the same condition. Comparing figures 13(a) and (c) shows that carbon monoxide emission index was reduced from 170 grams per kilogram of fuel (model 6A, fig. 13(c)) to 91 grams per kilogram fuel (model 6D, fig. 13(a)) by using radial fuel staging and variable combustor geometry at a fuel-air ratio of 0.0095.

Oxides of nitrogen. - The oxides-of-nitrogen emission index remained below 1.35 grams per kilogram of fuel for all models and test conditions covered. Model 6A had the lowest oxides-of-nitrogen emission index of 0.72 gram per kilogram of fuel with combustion in both annuli. Because of the low inlet-air temperature and pressure and low exit temperature, oxides of nitrogen became an insignificant exhaust emission problem at the ground idle condition of this investigation.

## Exit Temperature Profile

Exit temperature profile at ground idle is not normally a significant design consideration because of the low fuel-air ratios and consequently low temperatures involved. However, when variable combustor geometry or radial fuel staging or both are used, normal exhaust dilution will likely not occur. Therefore, the exit temperature profile must be evaluated to determine if there is a problem of unusually high exit temperatures which could cause stator vane or turbine deterioration.

Model 6C, the model with the highest combustion efficiency with radial fuel staging, also had the highest average radial and peak exit temperatures. Table III lists these temperatures at idle for combustion in both annuli, in the inner annulus only, and in the outer annulus only for models 6C and 6A. The table also gives the average radial and peak temperatures encountered at takeoff and cruise for the unmodified combustor, model 6A. Data for models 6B and 6D are not given in table III because their highest average radial exit and peak exit temperatures fell between those of models 6A and 6C. The data show that with radial fuel staging to the inner annulus only, the peak exit temperatures approach those of takeoff and Mach 3.0 cruise. However, these temperatures should result in minimal turbine cooling problems because of the relatively cold combustor inlet air available for stator and turbine cooling at idle.

## Combustor Total-Pressure Loss

Table IV shows the combustor total-pressure loss including the diffuser loss for the combustor models tested. It should be noted that all models will have a pressure loss comparable to that of model 6A upon acceleration from idle once the variable-geometry components have moved to their nonidle position. Model 6C, the model with the lowest overall exhaust emissions, shows a moderate 0.6-percentage-point increase in pressure loss above the 4.6-percent pressure loss of model 6A.

## Effects of Preheated Fuel

Combustion efficiency of model 6C was increased substantially, from 77.0 to 89.8 percent, at a fuel-air ratio of 0.008 with combustion in both annuli when 410 K fuel was used in place of ambient-temperature fuel. However, when radial fuel staging was used with combustion in the inner annulus only at an overall fuel-air ratio of 0.008, 410 K fuel increased combustion efficiency by only 0.1 percentage point, from 93.2 to 93.3 percent. Peak exit temperatures decreased slightly when the 410 K fuel was used.

## Durability

The unmodified combustor, model 6A, experienced no durability problems. All the simulated variable-geometry models experienced damage to the outer liner primary-zone scoops except when combustion was maintained in the inner annulus only. The damage to the outer liner primary scoops resulted from the fact that these scoops received their airflow solely from the total pressure head available. The static pressure was nearly equal on both sides of the outer liner in the region of the primary scoops. Therefore, slight airflow disturbances were sufficient to cause momentary interruptions in airflow through these scoops with resultant overheating and damage. Therefore, it is necessary to confine combustion to the inner annulus only with these types of variable-geometry modifications whenever the combustors are in the idle geometry configuration or redesign the outer liner shroud to increase airflow to the outer primary scoops. Redesign of the outer liner primary scoops may also be necessary.

Table V summarizes the airflow distribution between the combustor shrouds as defined in figure 1. This table shows that about 30 to 40 percent less air flows in the outer shroud air passage than in the inner. If the outer liner air shroud were extended upstream a few millimeters, the inner and outer shroud flows could be brought into balance without reducing the bypass flow significantly. It should be noted that five to eight times as much flow is bypassed than is needed to increase the outer shroud flows to bring them into balance with the inner shroud flows. This modification would likely stop the outer liner scoop damage that was encountered with combustion in the outer annulus only. The resulting reduction in bypass air from this modification may increase exhaust emissions. However, since the outer annulus is more lightly loaded (lower space heating rate) than the inner annulus, exhaust emissions may continue to decrease even with the reduced bypass flow. And, of course, the peak exit temperatures are small with combustion in the outer annulus only compared with those with combustion in the inner annulus only, as indicated in table III.

## SUMMARY OF RESULTS

Significant improvements in low-pressure-ratio engine combustor ground idle performance were obtained by utilizing variable combustor geometry and radial fuel staging. A simulated variable geometry combustor model with a translating outer exit transition liner and an inlet velocity profile distorted toward the outer diameter (model 6C) increased combustion efficiency to 95.2 percent at an overall fuel-air ratio of 0.01 with combustion in the inner annulus only. This efficiency compared with only 88.6 percent at the same operating condition for the unmodified combustor (model 6A) with combustion in the same annulus. Exhaust emissions of unburned hydrocarbons and carbon monoxide decreased significantly as a result of this improvement in combustion efficiency.

The tests demonstrated the potential of variable combustor geometry in conjunction with radial fuel staging to aid in meeting Environmental Protection Agency exhaust emission standards.

Exit temperature profile, though greatly increased in severity because of radial fuel staging, remained within acceptable levels. Total-pressure loss increased 0.6 percentage point with model 6C compared with model 6A.

Lewis Research Center,
National Aeronautics and Space Administration,
Cleveland, Ohio, October 16, 1974,
505-04.

## REFERENCES

1. Environmental Protection Agency - Control of Air Pollution From Aircraft and Aircraft Engines - Emission Standards and Test Procedures for Aircraft. Federal Register, vol. 38, no. 136, pt. 2, Tuesday, July 17, 1973, pp. 19088-19103.

2. Schultz, Donald F.: Modifications That Improve Performance of a Double Annular Combustor at Simulated Engine Idle Conditions. NASA TM X-3127, 1974.

3. Ingebo, Robert D.; and Norgren, Carl T.: Performance and Durability of Improved Air-Atomizing Splash-Cone Fuel Nozzles. NASA TM X-3156, 1974.

4. Schultz, Donald F.: Variable Combustor Geometry for Improving the Altitude Relight Capability of a Double Annular Combustor. NASA TM X-3163, 1974.

5. Perkins, Porter J.; Schultz, Donald F.; and Wear, Jerrold D.: Full-Scale Tests of a Short-Length, Double-Annular Ram Induction Turbojet Combustor for Supersonic Flight. NASA TN D-6254, 1971.

6. Schultz, Donald F.: Exhaust Emissions of a Double Annular Combustor - Parametric Study. NASA TM X-3164, 1974.

7. Juhasz, Albert J.: Performance of an Asymmetric Short Annular Diffuser with a Nondiverging Inner Wall Using Suction. NASA TN D-7575, 1974.

8. Central Automatic Data Processing System. NACA TN 4212, 1958.

9. Mealey, Charles; and Kee, Leslie: A Computer-Controlled Central Digital Data Acquisition System. NASA TN D-3904, 1967.

10. Glawe, George E.; Simmons, Frederick S.; and Stickney, Truman M.: Radiation and Recovery Corrections and Time Constants of Several Chromel-Alumel Thermocouple Probes in High-Temperature, High-Velocity Gas Streams. NACA TN 3766, 1956.

11. Rusnak, J. P.; and Shadowen, J. H.: Development of an Advanced Annular Combustor. (PWA-FR-2832, Pratt & Whitney Aircraft.) NASA CR-72453, 1969.

12. Schultz, Donald F.: Effect of Design Features on Performance on a Double-Annular Ram Induction Combustor. NASA TN D-7878, 1975.

TABLE I. - COMBUSTOR CONFIGURATIONS TESTED

| Model | Swirler | Transition liner | Snout blockage, percent | Inlet-airflow distortion |
|---|---|---|---|---|
| 6A | Radial | Standard | None | None |
| 6B | Radial | Short | 75 | None |
| 6C | Radial | ↓ | None | Tip-peaked |
| 6D | Axial | | 75 | ↓ |
| 6E[a] | Radial | | None | |
| 6F[a] | Radial | | 58 | |
| 6G[a] | Radial | | 25 | |

[a]Combustor performance was poor and is not presented in detail in this report.

TABLE II

| Run | Model | Inlet-air conditions | | | | | Combustor operating conditions | | | | | Annulus supplied with fuel |
|---|---|---|---|---|---|---|---|---|---|---|---|---|
| | | Velocity profile | Total pressure, $N/cm^2$ | Total temperature, K | Airflow kg/sec | Diffuser inlet Mach number | Reference velocity, m/sec | Fuel-air ratio | Average outlet temperature, K | Inlet fuel temperature, K | Fuel nozzle differential pressure, $N/cm^2$ | |
| 940 | 6A | Flat | 19.8 | 372 | 18.3 | 0.222 | 23.0 | 0.010 | 673 | 290 | 180 | Both |
| 944 | ↓ | ↓ | 19.8 | 360 | 19.5 | .223 | 22.7 | .0119 | 748 | 291 | 275 | Both |
| 945 | | | 19.9 | 359 | 18.7 | .222 | 22.6 | .008 | 446 | 291 | 114 | Both |
| 946 | | | 19.9 | 358 | 18.6 | .221 | 22.4 | .008 | 632 | 291 | 507 | Inner onl |
| 947 | | | 19.9 | 361 | 18.5 | .221 | 22.5 | .0096 | 690 | 293 | 743 | Inner onl |
| 948 | | | 20.0 | 364 | 18.4 | .219 | 22.5 | .0099 | 708 | 295 | 747 | Outer onl |
| 949 | | | 19.8 | 365 | 18.5 | .222 | 22.8 | .0082 | 648 | 295 | 475 | Outer onl |
| 950 | | | 19.8 | 365 | 18.5 | .222 | 22.8 | .008 | 641 | 408 | 581 | Outer onl |
| 966 | | | 19.9 | 370 | 18.3 | .222 | 22.8 | .0082 | 534 | 300 | 115 | Both |
| 981 | 6C | Tip-peaked | 19.8 | 367 | 18.2 | 0.228 | 22.7 | 0.0121 | 797 | 291 | 263 | Both |
| 983 | ↓ | ↓ | 19.8 | 367 | 18.3 | .229 | 22.7 | .0102 | 712 | 292 | 180 | Both |
| 984 | | | 19.6 | 368 | 18.1 | .229 | 22.7 | .0082 | 597 | 292 | 111 | Both |
| 986 | | | 19.7 | 369 | 18.0 | .227 | 22.6 | .0082 | 660 | 293 | 515 | Inner onl |
| 987 | | | 19.8 | 370 | 18.2 | .228 | 22.7 | .0096 | 721 | 294 | 741 | Inner onl |
| 989 | | | 19.8 | 372 | 18.2 | .228 | 22.9 | .0101 | 750 | 295 | 729 | Outer onl |
| 999 | | | 19.7 | 369 | 18.1 | .227 | 22.6 | .0082 | 660 | 407 | 135 | Both |
| 1000 | | | 19.4 | 370 | 18.1 | .232 | 23.0 | .0083 | 667 | 414 | 615 | Inner onl |
| 1001 | | | 19.5 | 370 | 18.1 | .230 | 22.9 | .0081 | 675 | 414 | 567 | Outer onl |
| 1149 | 6D | Flat | 20.0 | 368 | 18.3 | 0.221 | 22.7 | 0.0081 | 586 | 300 | 119 | Both |
| 1151 | ↓ | ↓ | 20.0 | 366 | 18.3 | .219 | 22.4 | .0101 | 721 | 299 | 190 | Both |
| 1152 | | | 20.1 | 366 | 18.2 | .218 | 22.2 | .0122 | 455 | 300 | 284 | Both |
| 1156 | | | 20.0 | 367 | 18.3 | .218 | 22.3 | .0095 | 731 | 301 | 755 | Inner onl |
| 1158 | | | 20.0 | 368 | 18.3 | .220 | 22.5 | .008 | 675 | 417 | 633 | Inner onl |
| 1523 | 6B | Flat | 20.7 | 370 | 18.1 | 0.211 | 21.7 | 0.0083 | 664 | 294 | 105 | Both |
| 1524 | ↓ | ↓ | 20.5 | 375 | 18.2 | .215 | 22.3 | .0083 | 666 | ↓ | 105 | ↓ |
| 1525 | | | 20.6 | 373 | 18.7 | .220 | 22.7 | .010 | 745 | | 170 | |
| 1526 | | | 20.7 | 369 | 18.9 | .220 | 22.5 | .0099 | 737 | | 170 | |
| 1551 | | | 20.4 | 369 | 17.9 | .211 | 21.8 | .0084 | 644 | 282 | 100 | |
| 1552 | | | 20.1 | 370 | 18.2 | .214 | 22.2 | .0104 | 748 | 284 | 164 | |
| 1553 | | | 20.3 | 369 | 17.9 | .213 | 22.1 | .0124 | 835 | 285 | 240 | |
| 1554 | | | 20.4 | 369 | 18.1 | .212 | 21.9 | .0081 | 665 | 286 | 447 | Inner onl |
| 1555 | | | 20.2 | 369 | 18.2 | .215 | 22.3 | .0102 | 746 | 287 | 737 | Inner onl |
| 1556 | | | 20.3 | 370 | 18.1 | .213 | 22.1 | .0083 | 683 | 288 | 435 | Outer onl |
| 1557 | ↓ | ↓ | 20.3 | 370 | 18.2 | .215 | 22.2 | .0102 | 753 | 289 | 690 | Outer onl |

TEST DATA

| Combustor performance characteristics | | | | | | | | | | |
|---|---|---|---|---|---|---|---|---|---|---|
| Pattern factor | Stator factor | Rotor factor | Combustor average temperature rise, K | Combustor pressure loss, percent | Combustion efficiency (by thermocouples) | Combustion efficiency (by exhaust analysis) | Oxides-of-nitrogen emission index, g $NO_x$/kg fuel | Carbon monoxide emission index, g CO/kg fuel | Hydrocarbon emission index, g $CH_2$/kg fuel | Ratio of gas-analysis to metered fuel-air ratio |
| 0.43 | 0.376 | 0.004 | 301 | 4.47 | 74.2 | 77.7 | 0.72 | 169.3 | 183.3 | 0.957 |
| .522 | .451 | .007 | 387 | 4.80 | 82.8 | 81.1 | .80 | 185.9 | 145.8 | 1.030 |
| .675 | .761 | .254 | 144 | 4.55 | 44.5 | 54.4 | .82 | 180.1 | 413.6 | 1.017 |
| 1.18 | 1.17 | .60 | 274 | 4.60 | 84.5 | 86.9 | .96 | 184.5 | 88.3 | 1.112 |
| 1.28 | 1.27 | .55 | 329 | 4.67 | 85.7 | 88.6 | .94 | 167.9 | 74.9 | 1.05 |
| 1.81 | 1.71 | .35 | 344 | 4.54 | 86.6 | 92.2 | .97 | 136.4 | 45.9 | .905 |
| 1.54 | 1.42 | .33 | 284 | 4.59 | 85.7 | 91.2 | 1.13 | 156.5 | 51.4 | .941 |
| 1.38 | 1.26 | .34 | 276 | 4.69 | 84.7 | 92.4 | .61 | 124.3 | 46.4 | .867 |
| .61 | .810 | .188 | 164 | 4.67 | 50.1 | 56.0 | .47 | 160.8 | 402.1 | 1.039 |
| 0.80 | 0.879 | 0.189 | 429 | 5.24 | 91.9 | 92.7 | 0.84 | 120.3 | 44.9 | 0.984 |
| .85 | .941 | .239 | 345 | 5.22 | 86.8 | 89.4 | .95 | 127.0 | 76.4 | .993 |
| .87 | 1.046 | .315 | 229 | 5.18 | 70.2 | 77.0 | .90 | 153.9 | 193.5 | 1.011 |
| 2.40 | 2.54 | .938 | 291 | 5.33 | 98.4 | 93.2 | 1.12 | 115.8 | 40.9 | 1.003 |
| 2.29 | 2.40 | .929 | 351 | 5.18 | 102.9 | 95.2 | 1.09 | 103.1 | 24.3 | .994 |
| 1.07 | 1.07 | .144 | 378 | 5.10 | 94.2 | 95.3 | 1.18 | 95.3 | 24.4 | .949 |
| .718 | .856 | .292 | 291 | 5.19 | 87.6 | 89.8 | .77 | 121.0 | 73.4 | 1.012 |
| 2.34 | 2.47 | .931 | 297 | 5.47 | 89.3 | 93.3 | .74 | 116.6 | 39.3 | 1.026 |
| .882 | .838 | .106 | 305 | 5.37 | 92.7 | 94.8 | .86 | 95.4 | 29.6 | 1.00 |
| 0.84 | 0.87 | 0.342 | 218 | 7.04 | 68.5 | 70.8 | 0.78 | 136.3 | 260.4 | 1.013 |
| .720 | .712 | .357 | 354 | 6.98 | 88.0 | 87.0 | .89 | 113.4 | 103.0 | .998 |
| .67 | .67 | .349 | 455 | 6.99 | 98.1 | 93.4 | .93 | 90.0 | 45.2 | .987 |
| 1.42 | 1.43 | .637 | 364 | 6.89 | 95.2 | 94.8 | 1.04 | 91.5 | 30.2 | .96 |
| 1.32 | 1.34 | .622 | 307 | 6.97 | 95.1 | 94.9 | 1.12 | 121.6 | 36.2 | .981 |
| 0.67 | 0.77 | 0.309 | 294 | 6.06 | 87.7 | 83.6 | 0.79 | 138.3 | 131.7 | 0.91 |
| .66 | .76 | .312 | 291 | 6.33 | 86.9 | 83.7 | .84 | 157.6 | 125.7 | .951 |
| .69 | .68 | .291 | 372 | 6.63 | 93.8 | 90.7 | .91 | 138.5 | 61.0 | .914 |
| .71 | .71 | .289 | 369 | 6.63 | 93.3 | 90.5 | .89 | 142.8 | 61.5 | .81 |
| .645 | .759 | .348 | 275 | 6.16 | 81.0 | 81.8 | 1.17 | 150.4 | 146.5 | 1.027 |
| .731 | .724 | .338 | 378 | 6.43 | 91.6 | 90.5 | 1.35 | 138.9 | 62.5 | 1.016 |
| .716 | .710 | .330 | 466 | 6.20 | 96.7 | 94.3 | 1.42 | 115.6 | 29.4 | 1.017 |
| 1.72 | 1.71 | .675 | 296 | 6.19 | 98.2 | 89.5 | 1.32 | 152.7 | 69.1 | 1.037 |
| 1.70 | 1.69 | .646 | 377 | 6.22 | 102.1 | 92.1 | 1.17 | 121.4 | 50.6 | 1.010 |
| .72 | .63 | .135 | 314 | 6.24 | 94.9 | 92.2 | 1.20 | 103.2 | 53.4 | .949 |
| .84 | .77 | .137 | 384 | 6.28 | 95.4 | 93.1 | 1.15 | 114.1 | 41.8 | .960 |

TABLE III. - COMPARISON PEAK EXIT TEMPERATURES

| Simulated test condition | Model | Annulus supplied with fuel | Overall fuel-air ratio | Highest average radial temperature, K | Peak exit temperature, K | Ideal average exit temperature, K (a) |
|---|---|---|---|---|---|---|
| Engine idle | 6A | Both | 0.01 | 684 | 800 | 735 |
| | 6C | Both | ↓ | 780 | 998 | ↓ |
| | 6A | Inner | | 860 | 1108 | |
| | 6C | Inner | | 1006 | 1521 | |
| | 6A | Outer | | 856 | 1326 | |
| | 6C | Outer | | 840 | 1145 | |
| Takeoff[b] | 6A | Both | 0.0258 | 1514 | 1641 | 1478 |
| Mach 3.0 cruise[b] | 6A | Both | .0172 | 1502 | 1586 | 1478 |

[a]Actual average exit temperature is less than this value when combustion efficiency is less than 100 percent.

[b]From ref. 12.

TABLE IV. - TOTAL-PRESSURE LOSS

INCLUDING DIFFUSER LOSS

[Inlet total pressure, 20.2 N/cm$^2$; inlet temperature, 367 K; reference velocity, 23 m/sec; overall fuel-air ratio, 0.008; diffuser inlet Mach number, 0.225.]

| Model | Total-pressure loss, percent |
|---|---|
| 6A | 4.6 |
| 6B | 6.1 |
| 6C | 5.2 |
| 6D | 7.1 |

TABLE V. - COMBUSTOR SHROUD

AIRFLOW DISTRIBUTIONS

[No data available for model 6C.]

| Model | To bypass passage | To outer passage | To center passage | To inner passage |
|---|---|---|---|---|
| | Airflow, percent | | | |
| 6A | 2.0 | 26.2 | 49.2 | 22.6 |
| 6B | 39.8 | 9.8 | 36.3 | 14.1 |
| 6D | 44.2 | 10.7 | 26.4 | 18.7 |

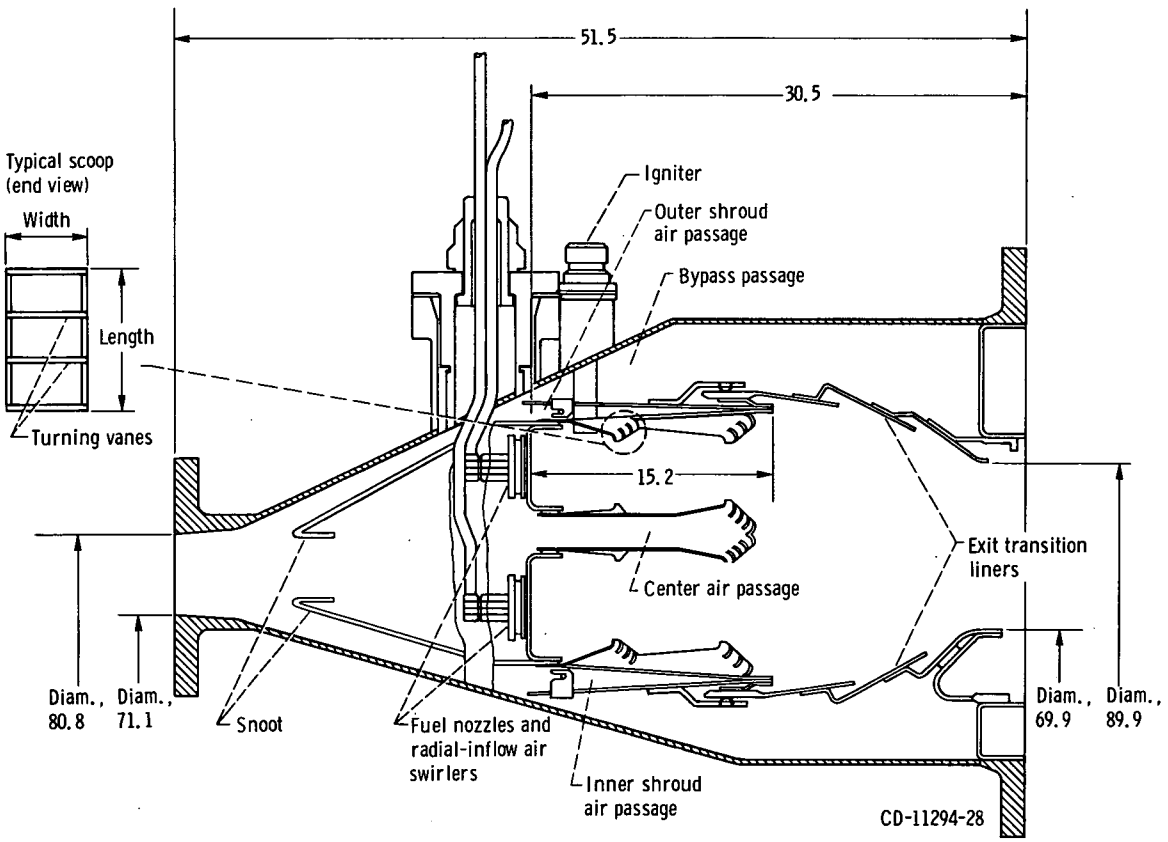


Figure 1. - Cross-sectional sketch of double-annular ram-induction combustor. (Dimensions are in centimeters.)

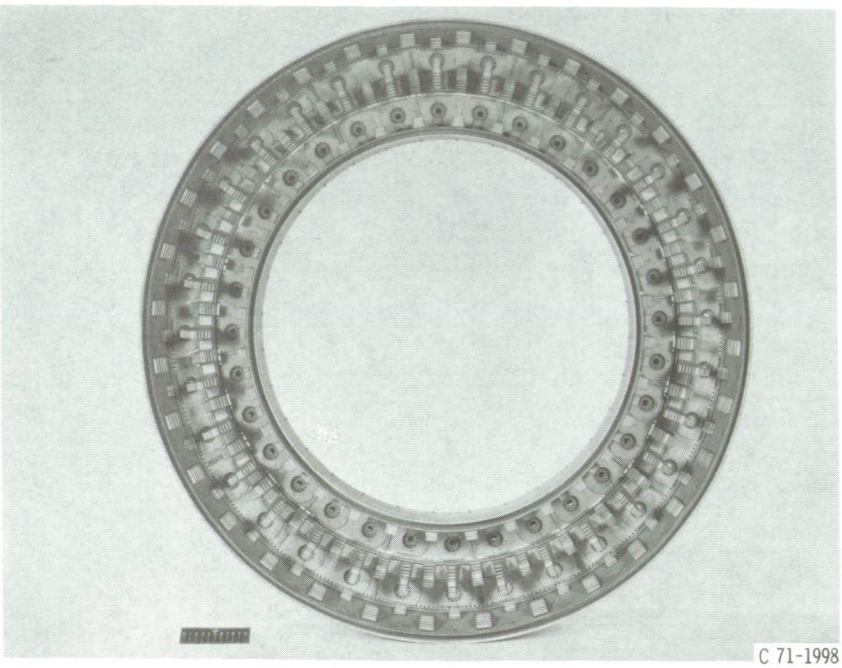


(a) View looking upstream.

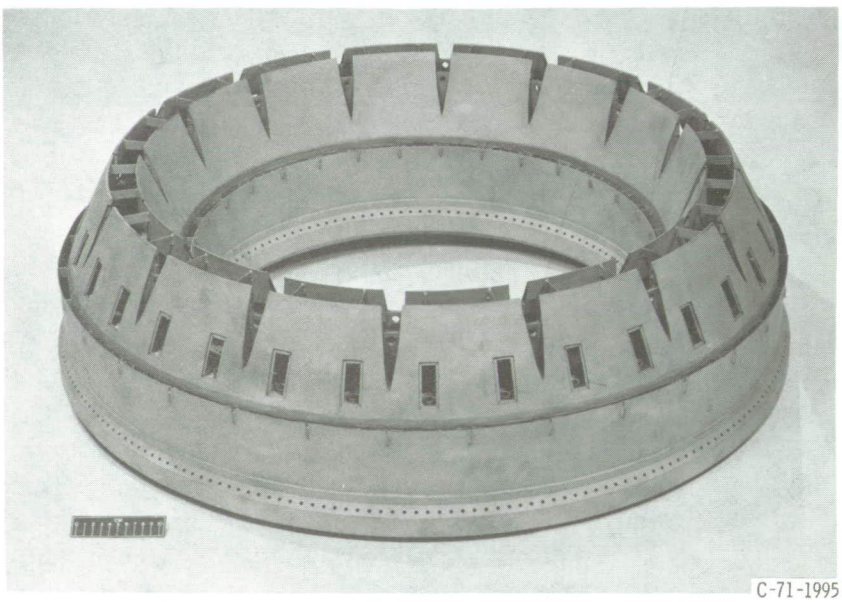


(b) View looking downstream outside.

Figure 2. - Test combustor in nonidle configuration with exit transition liners removed.

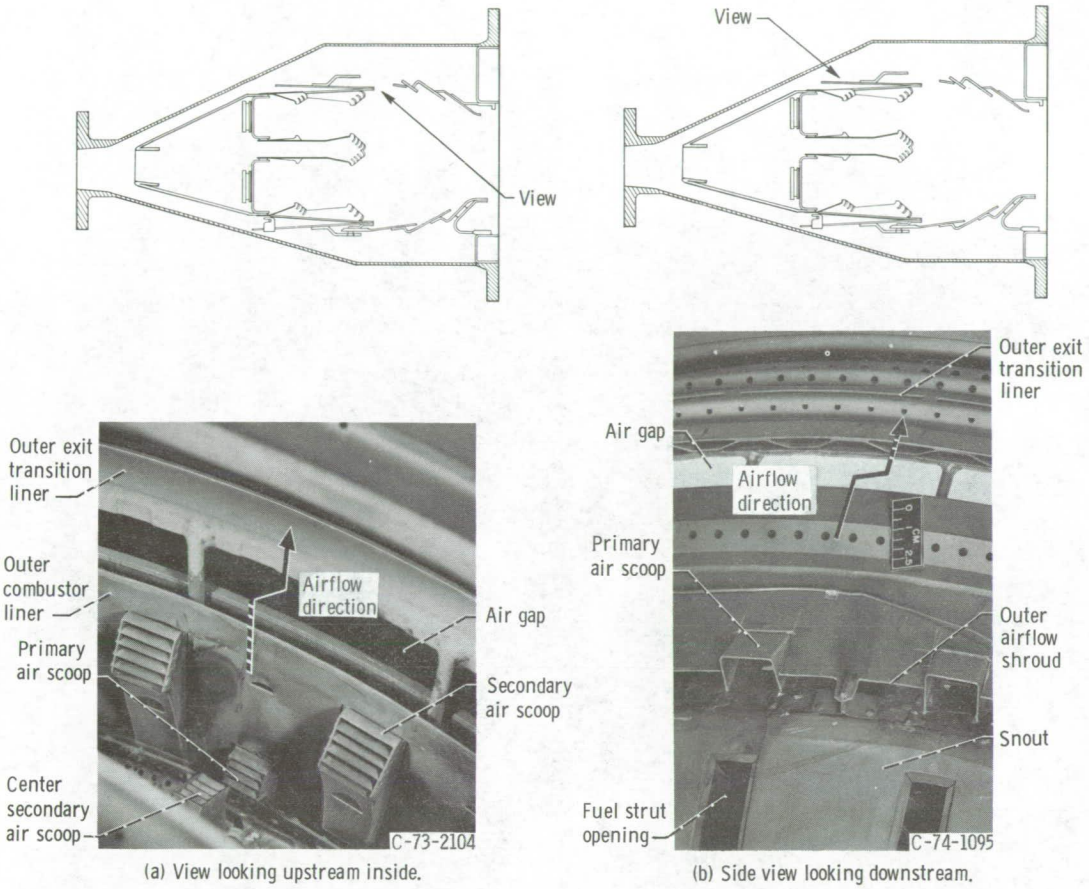


(a) View looking upstream inside.

(b) Side view looking downstream.

Figure 3. - Simulated variable-geometry exit transition liner in open idle position.

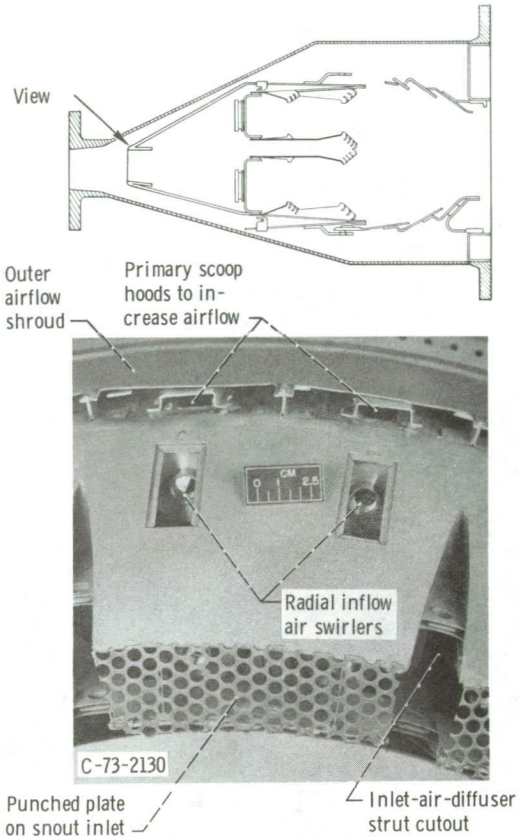


Figure 4. - Simulated variable-geometry snout blockage using punched plates welded to snout inlet.

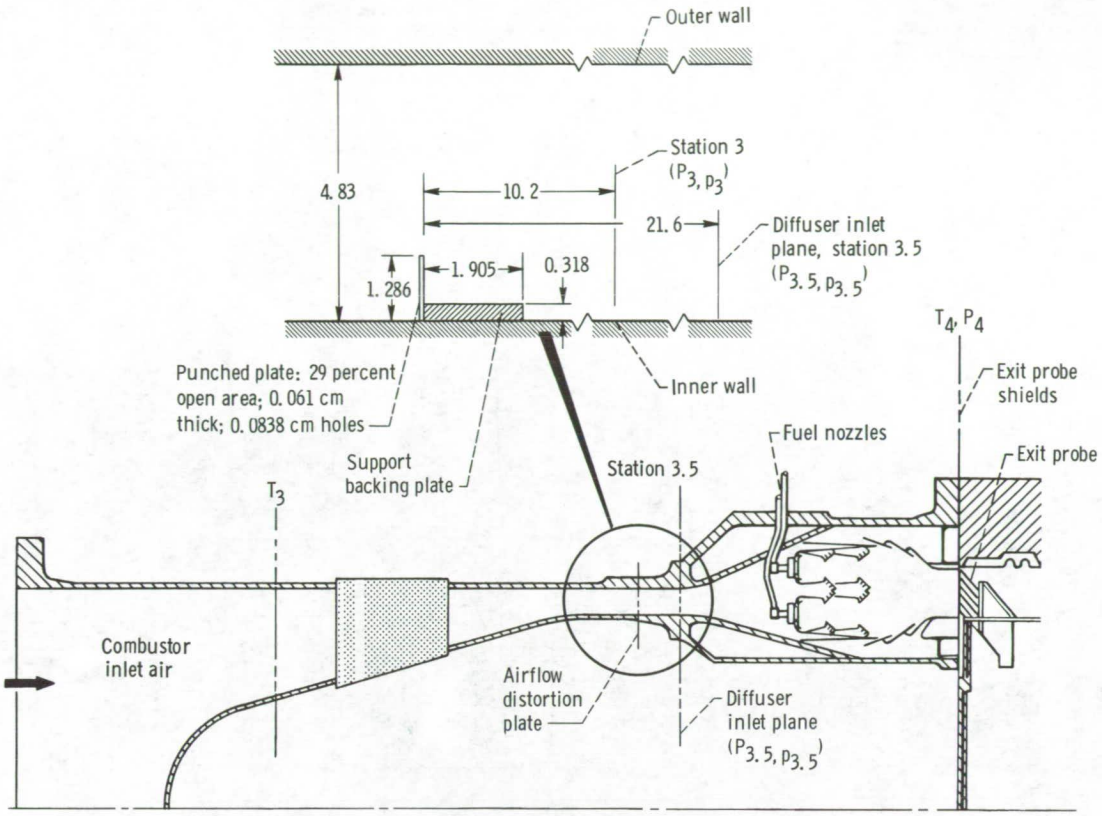


(a) Cross-sectional view showing axial location of plate. (Dimensions are in centimeters.)

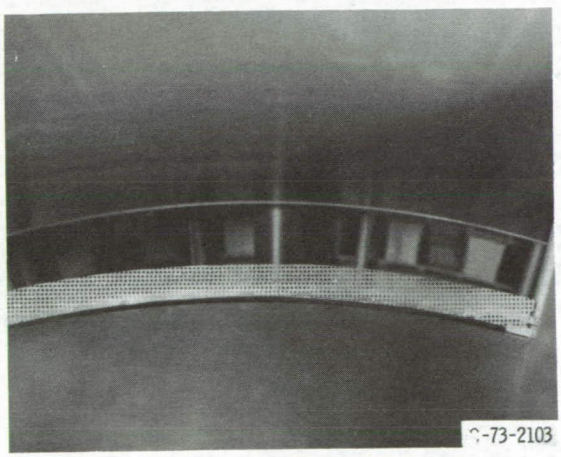


(b) View of plate looking downstream.

Figure 5. - Views of diffuser inlet airflow distortion plate used to simulate a tip-peaked compressor exit airflow profile and plot of resulting airflow profile.

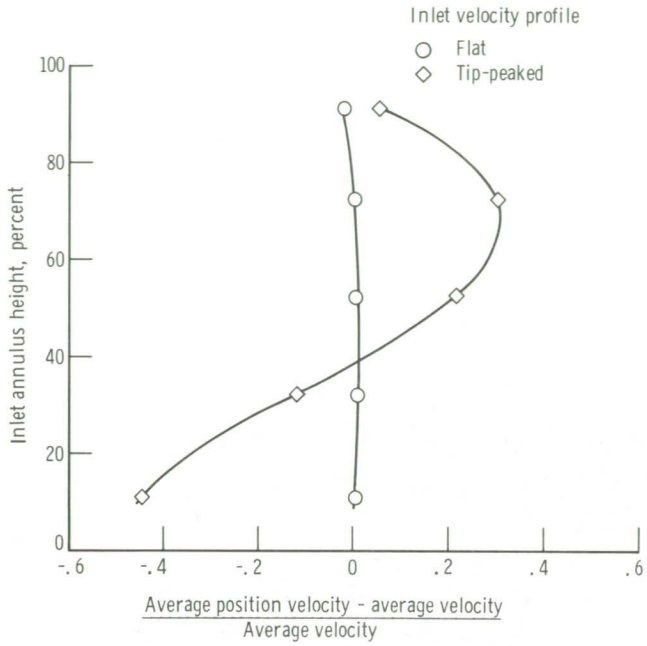


(c) Airflow profile resulting from use of plate. Simulated takeoff; inlet-air conditions: total pressure, 62 newtons per square centimeter; total temperature, 589 K; reference velocity, 30.5 meters per second; average velocity, 115 meters per second; Mach number, 0.243.

Figure 5. - Concluded.

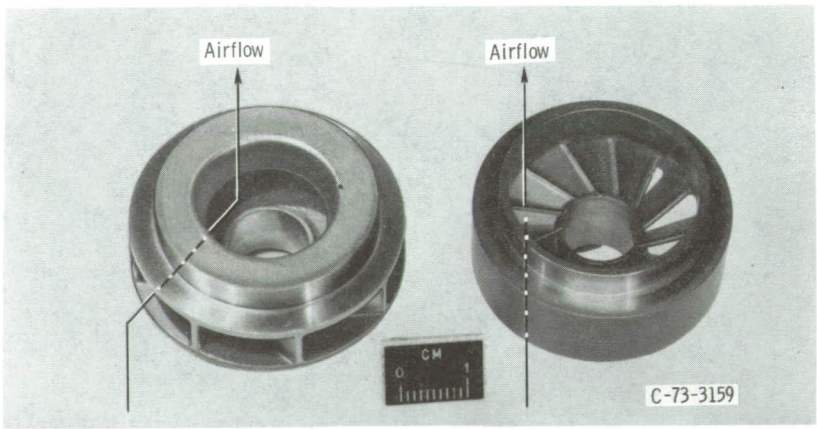


(a) Radial inflow.

(b) Axial flow.

Figure 6. - Comparison of radial inflow and axial-flow air swirlers used in this study.

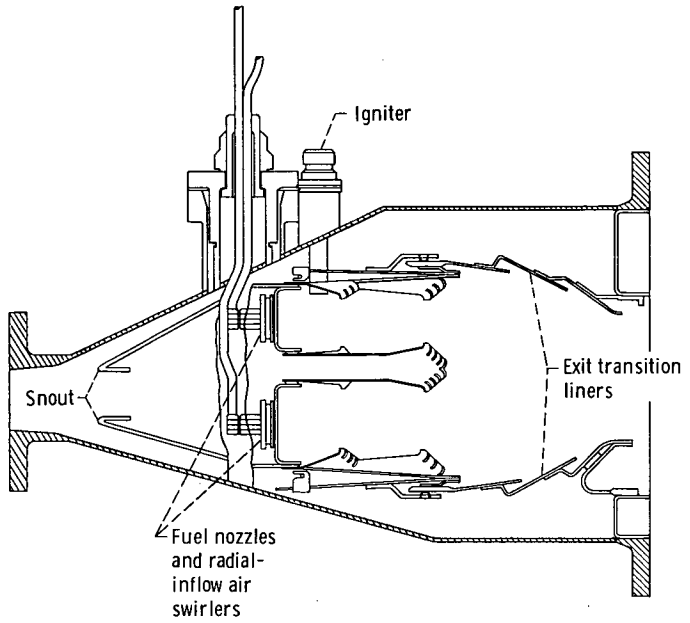


(a) Model 6A (unmodified combustor).

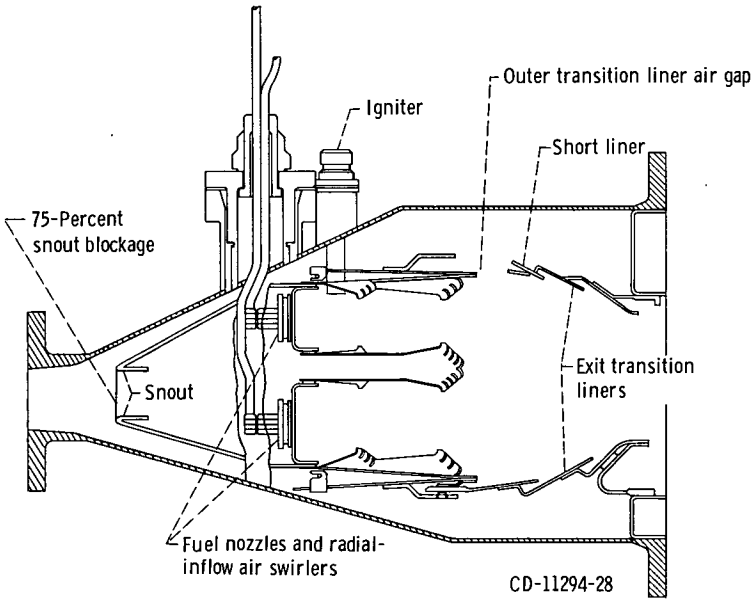


(b) Model 6B (short liner and snout blockage).

Figure 7. - Combustor configurations tested.

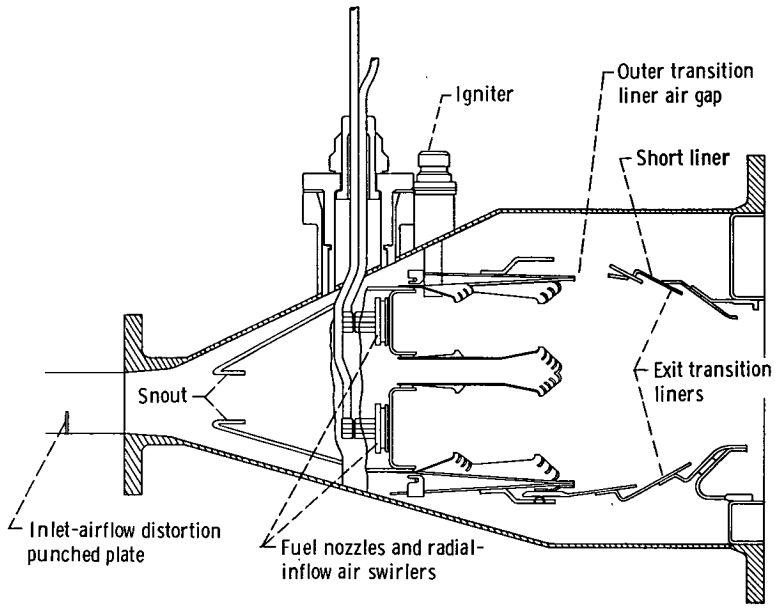


(c) Model 6C (short liner and inlet-air distortion).

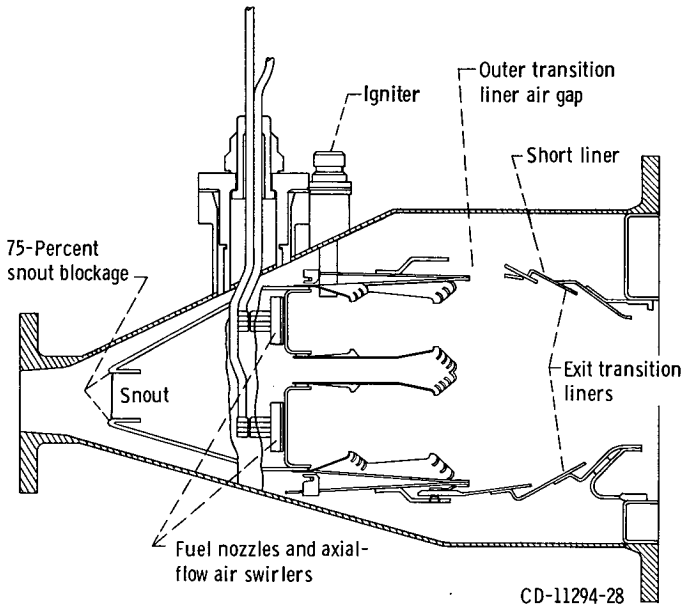


(d) Model 6D (short liner, snout blockage, and axial-flow air swirlers).

Figure 7. - Concluded.

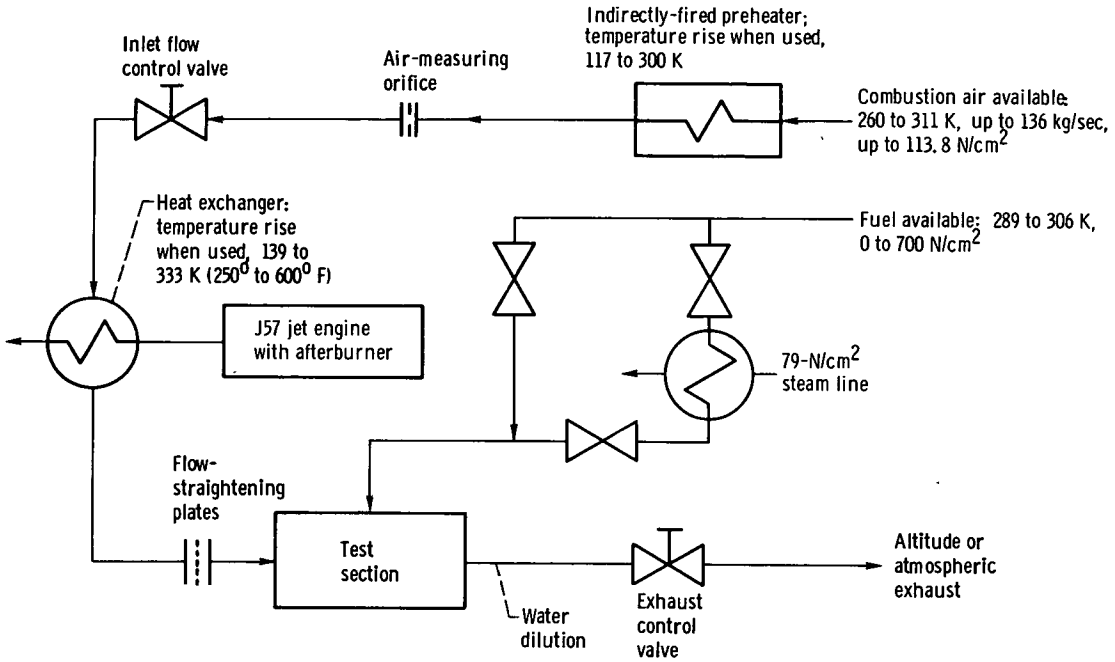


Figure 8. - Schematic of test facility combustion air and fuel.

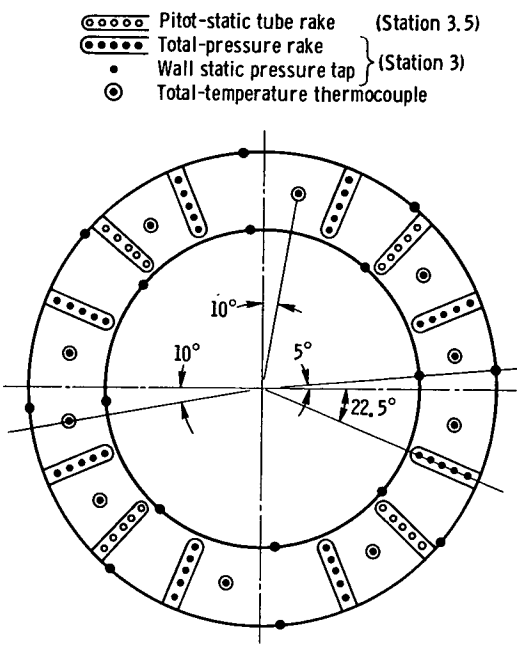


Figure 9. - Diffuser inlet instrumentation at station 3. View looking downstream.

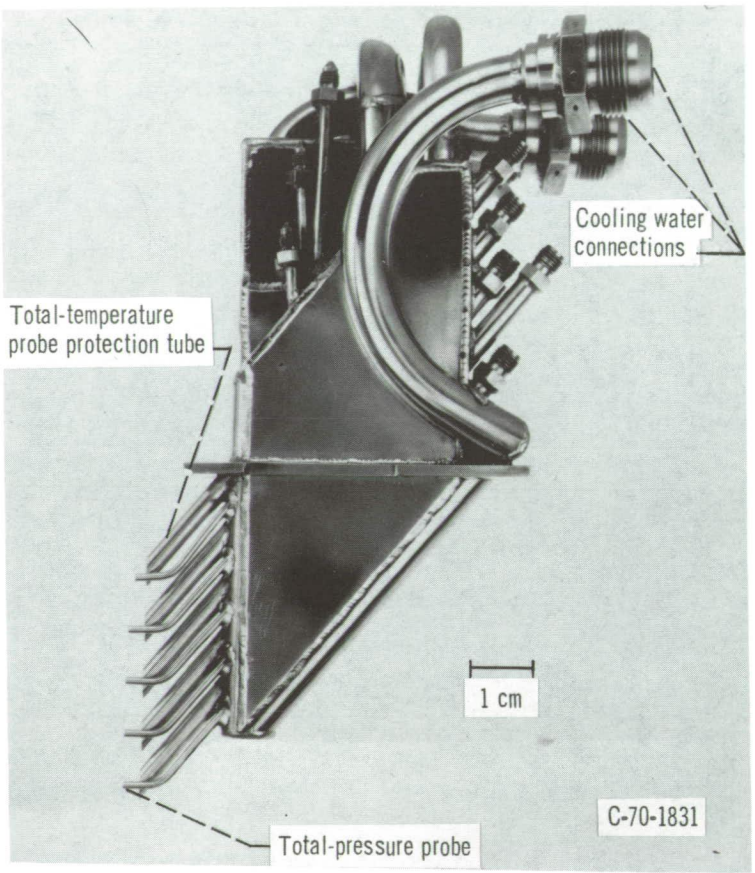


Figure 10. - Five-point total-temperature and total-pressure water cooled probe assembly.

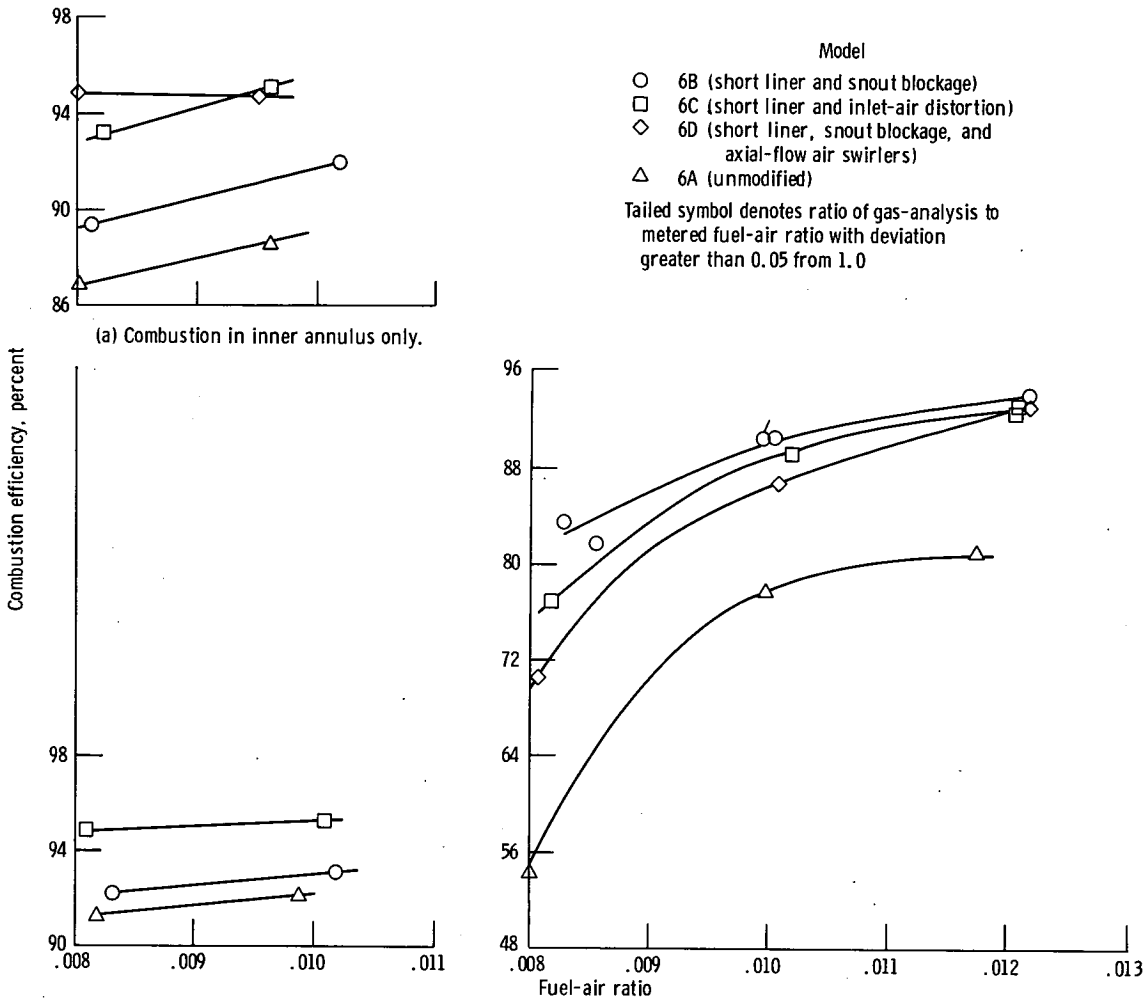


Figure 11. - Combustion efficiency as function of fuel-air ratio. Inlet total pressure, 20.2 newtons per square centimeter; inlet temperature, 367 K; reference velocity, 23 meters per second.

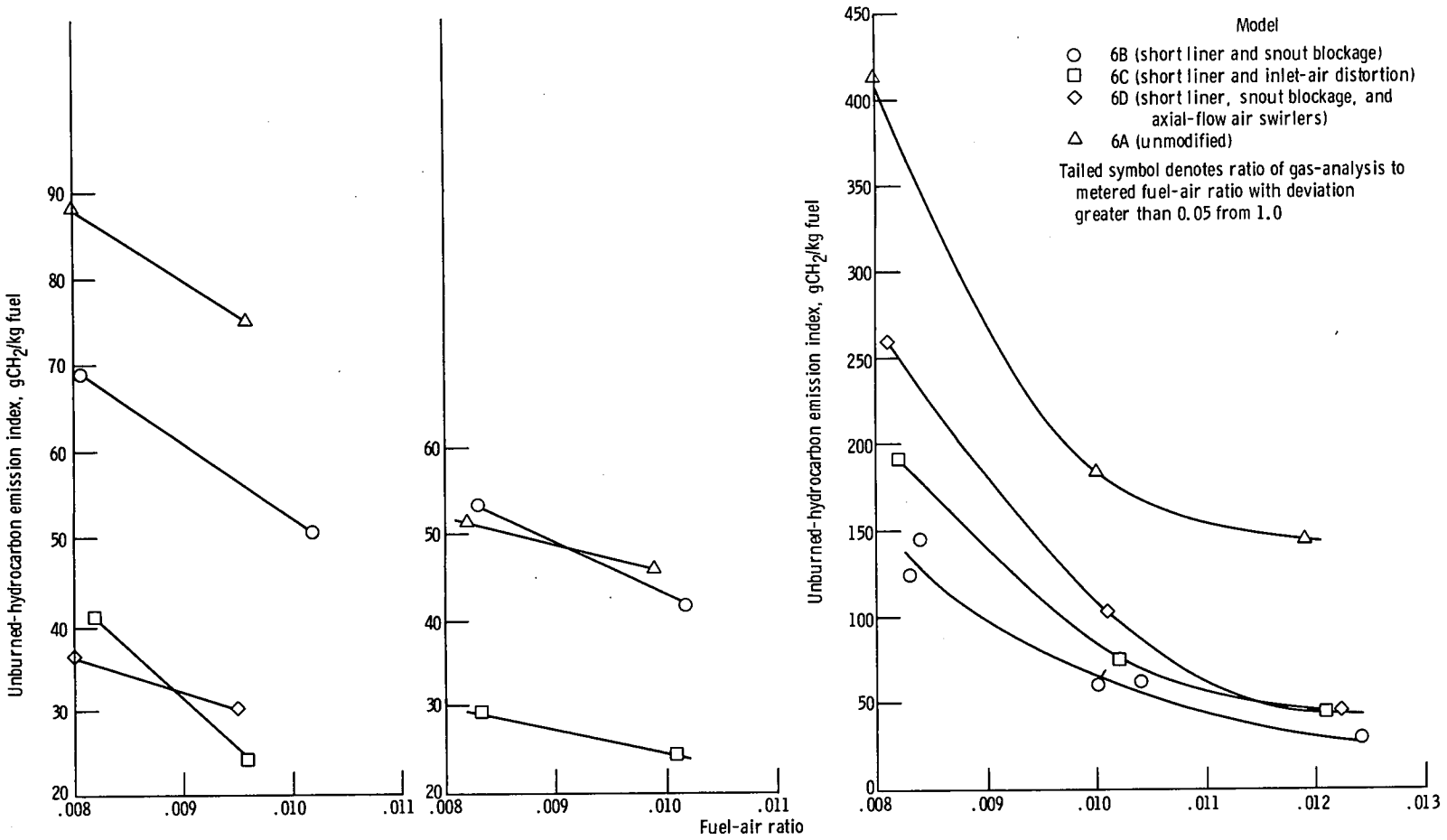


(a) Combustion in inner annulus only. (b) Combustion in outer annulus only. (c) Combustion in both annuli.

Figure 12. - Unburned-hydrocarbon emission index as function of fuel-air ratio. Inlet total pressure, 20.2 newtons per square centimeter; inlet temperature, 367; reference velocity, 23 meters per second.

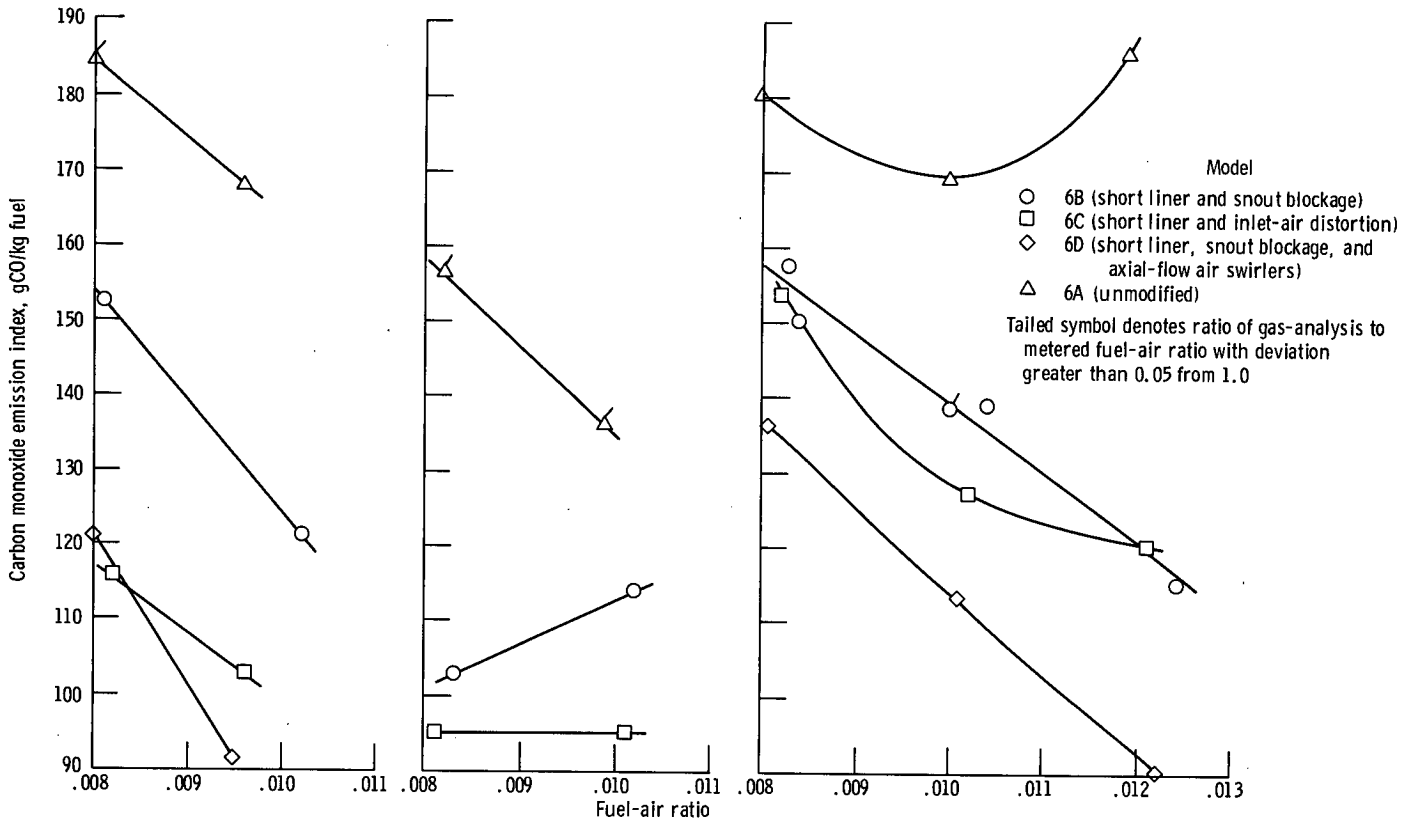


(a) Combustion in inner annulus only.

(b) Combustion in outer annulus only.

(c) Combustion in both annuli.

Figure 13. - Carbon monoxide emission index as function of fuel-air ratio. Inlet total pressure, 20.2 newtons per square centimeter; inlet temperature, 367 K; reference velocity, 23 meters per second.

NATIONAL AERONAUTICS AND SPACE ADMINISTRATION
WASHINGTON, D.C. 20546

OFFICIAL BUSINESS
PENALTY FOR PRIVATE USE $300

SPECIAL FOURTH-CLASS RATE
BOOK

POSTAGE AND FEES PAID
NATIONAL AERONAUTICS AND
SPACE ADMINISTRATION
451

U.S.MAIL

POSTMASTER: If Undeliverable (Section 158 Postal Manual) Do Not Return

*"The aeronautical and space activities of the United States shall be conducted so as to contribute . . . to the expansion of human knowledge of phenomena in the atmosphere and space. The Administration shall provide for the widest practicable and appropriate dissemination of information concerning its activities and the results thereof."*

—NATIONAL AERONAUTICS AND SPACE ACT OF 1958

# NASA SCIENTIFIC AND TECHNICAL PUBLICATIONS

TECHNICAL REPORTS: Scientific and technical information considered important, complete, and a lasting contribution to existing knowledge.

TECHNICAL NOTES: Information less broad in scope but nevertheless of importance as a contribution to existing knowledge.

TECHNICAL MEMORANDUMS: Information receiving limited distribution because of preliminary data, security classification, or other reasons. Also includes conference proceedings with either limited or unlimited distribution.

CONTRACTOR REPORTS: Scientific and technical information generated under a NASA contract or grant and considered an important contribution to existing knowledge.

TECHNICAL TRANSLATIONS: Information published in a foreign language considered to merit NASA distribution in English.

SPECIAL PUBLICATIONS: Information derived from or of value to NASA activities. Publications include final reports of major projects, monographs, data compilations, handbooks, sourcebooks, and special bibliographies.

TECHNOLOGY UTILIZATION PUBLICATIONS: Information on technology used by NASA that may be of particular interest in commercial and other non-aerospace applications. Publications include Tech Briefs, Technology Utilization Reports and Technology Surveys.

***Details on the availability of these publications may be obtained from:***

**SCIENTIFIC AND TECHNICAL INFORMATION OFFICE**

**NATIONAL AERONAUTICS AND SPACE ADMINISTRATION**

**Washington, D.C. 20546**